Available online at www.sciencedirect.com
SCIENCE DIRECT®
Journal of Hydrology 307 (2005) 164–174
Journal of Hydrology
www.elsevier.com/locate/jhydrol

Nonstationary hydrological time series forecasting using nonlinear dynamic methods

Paulin Coulibaly[a,*], Connely K. Baldwin[b]

[a]*Department of Civil Engineering/School of Geography and Geology, McMaster University, Hamilton, Ont., Canada L8S 4L7*
[b]*Utah Water Research Laboratory, Utah State University, Logan, UT 84322-8200, USA*

Received 24 October 2003; revised 30 August 2004; accepted 1 October 2004

Abstract

Recent evidence of nonstationary trends in water resources time series as result of natural and/or anthropogenic climate variability and change, has raised more interest in nonlinear dynamic system modeling methods. In this study, the effectiveness of dynamically driven recurrent neural networks (RNN) for complex time-varying water resources system modeling is investigated. An optimal dynamic RNN approach is proposed to directly forecast different nonstationary hydrological time series. The proposed method automatically selects the most optimally trained network in any case. The simulation performance of the dynamic RNN-based model is compared with the results obtained from optimal multivariate adaptive regression splines (MARS) models. It is shown that the dynamically driven RNN model can be a good alternative for the modeling of complex dynamics of a hydrological system, performing better than the MARS model on the three selected hydrological time series, namely the historical storage volumes of the Great Salt Lake, the Saint-Lawrence River flows, and the Nile River flows.

Keywords: Nonstationarity; Hydrologic time series; Modeling; Recurrent neural networks; Multivariate adaptive regression splines

1. Introduction

The prediction of environmental time series requires modeling of the underlying physical mechanism responsible of their generation. In practice, many of the real-world dynamical system signals exhibit two distinct characteristics: nonlinearity, and nonstationarity in the sense that statistical characteristics change over time due to either internal or external nonlinear dynamics. Explicit examples of such signals are the historical storage volumes of the Great Salt Lake (GSL), the Saint-Lawrence River (SLR) flow records, and the Nile River flow series. Large or regional hydro-systems are inherently dynamic and subject to climate variability and change. The evidence of nonstationarity of some existing long hydrological records has raised a number of questions as to the adequacy of the conventional statistical methods for long-term regional water resources forecasting. The fundamental assumption in most empirical or statistical approaches (Box and Jenkins, 1976) is stationarity over time. Therefore, nonstationary time series have

* Corresponding author. Fax: +1 905 529 9688.
E-mail address: couliba@mcmaster.ca (P. Coulibaly).

0022-1694/$ - see front matter © 2004 Elsevier B.V. All rights reserved.
doi:10.1016/j.jhydrol.2004.10.008

to be reduced to being stationary, for example through differencing. This procedure has the disadvantage of amplifying high frequency noise in the data (Young, 1999). The simplest alternatives to the linear regression methods are the dynamic regression models (Young, 1999). Although these methods may indeed be useful for the analysis of nonstationary time series, their inherently static regression feature cannot fully explain many complex geophysical datasets. The identification of a nonlinear dynamical model that relates directly to the underlying dynamics of the system being modeled remains a challenging and active research topic. Owing to the difficulty of identifying an appropriate nonlinear model structure, very few nonlinear empirical models have been proposed in the literature for complex hydrological time series modeling (Coulibaly et al., 2000a). In watershed and aquifer system modeling, recent attempts have resorted to nonlinear data-driven methods, specifically artificial neural networks (ANNs), which are found more suited to nonlinear input–output mapping. Recent reviews reveal that in more than 90% of the applications of artificial neural networks (ANNs) for water resources variables modeling, the standard feedforward neural networks (FNNs) have been used (Coulibaly et al., 1999; Maier and Dandy, 2000; ASCE Task Committee, 2000). Even though an optimal FNN model can provide accurate forecasts for simple rainfall-runoff problems, it often yields sub-optimal solutions even with lagged inputs or tapped delay lines (Coulibaly et al., 2001). Standard FNNs are not well suited for complex temporal sequences processing owing to their static memory structure (Giles et al., 1997; Haykin, 1999). FNNs are similar to nonlinear static regression models in that they are unable to adapt properly to the temporal relationship of real-world data. A promising class of ANNs for nonstationary time series modeling is the dynamically driven recurrent neural networks (RNNs) (Haykin and Li, 1995; Haykin, 1999). In theory, a RNN can learn the underlying dynamics of a nonstationary environment if the training sample is representative of the time-varying behavior of the system been modeled (Haykin, 1999). However, designing such a network for nonlinear prediction of physical nonstationary time series is a difficult task because (1) the traditional gradient-descent learning methods are unstable, and have to be properly adapted; and (2) the network needs to learn on-line and adapt to statistical variations of the time series while simultaneously performing its filtering role. Recent attempts in using RNNs for nonstationary time series prediction have demonstrated the potential of the method for modeling complex time-varying patterns (Saad et al., 1998; Iatrou et al., 1999; Coulibaly et al., 2000a). However, none of these applications has considered nonstationary hydrological time series.

The purpose of this paper is to introduce a dynamic RNN approach for the prediction of nonstationary hydrological time series. The proposed method uses an ensemble of parallel and competitive sub-networks (or 'subnets') to directly identify the optimal dynamic model for the system being considered. The performance of the method is assessed against that of an optimal multivariate adaptive regression splines (MARS) model (Friedman, 1991; Lall et al., 1996) in experiments based on complex hydrological series modeling for three physically different hydro-climatic regions.

The reminder of the paper is organized as follows. Section 2 provides a brief description of the experiment data, related studies, and our wavelet analyses of the data. In Section 3, we describe the dynamic RNN and the ensemble competition approach. In Section 4, results from the modeling experiment are reported and discussed. Finally, in Section 5, our conclusions are presented.

2. Experiment data and wavelet analyses

Three hydrological time series that have been analyzed extensively by numerous authors (Eltahir, 1996; Bernier, 1994; Sangoyomi, 1993) and whose statistical characteristics have been shown to change over time (i.e. corresponding to the term 'nonsta-nonstationary process' used here) are considered. These are; the monthly flow records of the Nile River at Aswan, from 1871 to 1989, the monthly discharges of the Saint-Lawrence River (SLR) at Cornwall, from 1861 to 1999, and the bi-weekly storage volumes of the Great Salt Lake (GSL), from 1847 to 1999. The selected hydrological series were also proven to exhibit significant linkages with low-frequency (inter-annual or decadal) climatic variability indices. It has

been reported that the underlying mean of the Nile river flow is both time and El-Niño/Southern Oscillation (ENSO) dependent, resulting in a nonstationary process (Eltahir, 1996). The changes in the mean of the SLR flows have been analyzed by Bernier (1994), who showed that the 1861–1991 annual flows of the SLR can be divided into three periods (1861–1891, 1892–1968, 1969–1991) with significantly different means. The nonlinear time-varying dynamics of the GSL have been documented by Sangoyomi (1993) and Lall et al. (1996). Furthermore, the connection between the climatic signals and the fluctuations in the volume of the GSL has been proven and is well documented by Lall and Mann (1995) and Mann et al. (1995). Fig. 1 shows the deviations from the historical mean for the three hydrological series under study. It appears that globally the selected time series exhibit long-term (greater than 10 years) as well as low-frequency (interannual to decadal) downward and/or upward trends in addition to the inherent seasonal fluctuations. Prior to the year 1900, there are essentially positive deviations from the historical mean of the series whereas after 1900, the negative deviations are relatively dominant up to 1999 except for the Saint-Lawrence River (SLR) flows (e.g. the period 1969–1999). More specifically, there are apparent periodical patterns in each series from 1900 onwards. These visual structures are supported by more rigorous statistical analysis (Lall and Mann, 1995; Eltahir, 1996; Bernier, 1994). Nevertheless, to further assess the complexity of the selected time series, a Morlet

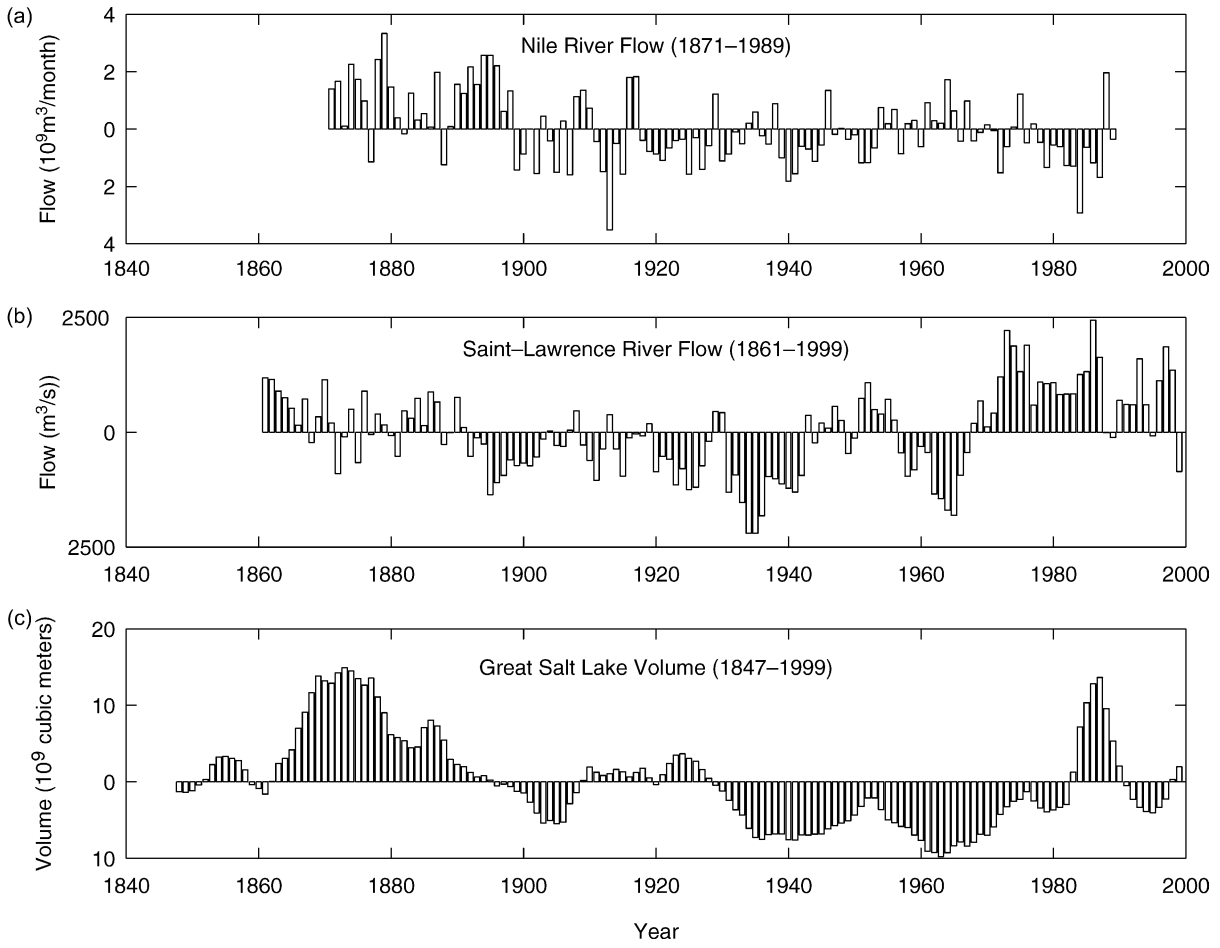

Fig. 1. Deviations of annual hydrological records from their historical means.

wavelet analysis of the selected hydrological time series is carried out.

Wavelet analysis. The theoretical basis for using the wavelet transform to analyze a time series that contains nonstationary power at different frequencies has been documented by Daubechies (1990). The Morlet wavelet is a complex nonorthogonal wavelet function which has been shown particularly adapted for analyzing nonstationary variance at different frequencies within hydrologic and geophysical time series (Foufoula-Georgiou and Kumar, 1995; Torrence and Campo, 1998; Coulibaly et al., 2000a; Labat et al., 2000). In this analysis, the wavelet analysis toolkit kindly provided by Torrence and Campo (1998) (at URL: http://paos.colorodo.edu/research/wavelets/) is used. With the wavelet analysis, localized time-scale variations can be seen within the GSL volume series (Fig. 2). It should be noted that only the structures (or components) corresponding to the highest wavelet coefficient are shown. The contour lines in Fig. 2b enclose structures of greater than 95% confidence for a red-noise process with a lag-1 coefficient of 0.98. In Fig. 2b, the Morlet wavelet power spectrum indicates distinct periodic processes (or components) characterized by a variable period (ranging from 0.5 year to 32 years). In addition to the persistent annual component, there are different multi-annual components. From 1870 to 1920, there is a clear shift from a period of around 4 years to a period of the order of 8–14 years (specifically from 1875 to 1920), while from 1920 to 1999, the shift is from longer to shorter periods. It also appears that larger

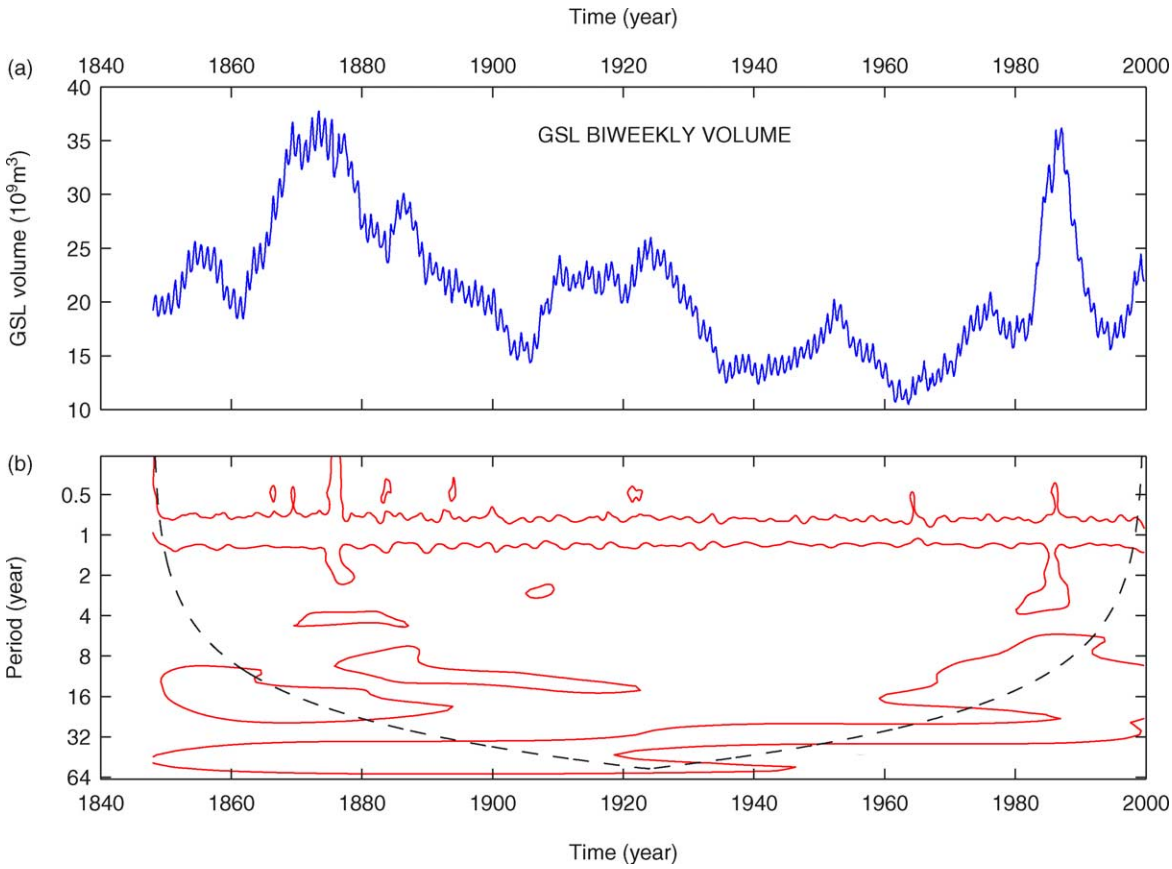

Fig. 2. (a) The GSL bi-weekly volume series used for the wavelet analysis. (b) The local wavelet power spectrum of (a) using the Morlet wavelet. The contours enclose structures of greater than 95% confidence for a red-noise process with a lag-1 coefficient of 0.98. The dashed curve depicts the cone of influence beyond which the edge effect become important.

GSL volumes ($>30\times10^9$ m^3) can be associated with the 2–4 year processes observed during 1870–1890 and 1985–1990 which in turn can be related to the strong El-Niño (ENSO) events observed at these time periods (Torrence and Campo, 1998).

Similarly, the Morlet wavelet spectra for the Saint-Lawrence and the Nile River flows are depicted in Fig. 3. The contour lines in Fig. 3a and b enclose structures of greater than 95% confidence for a red-noise process with a lag-1 coefficient of 0.90 and 0.61 for the Nile and the SLR monthly flows, respectively. The wavelet power spectra reveal more localized (in time) processes specifically before the year 1920, while from 1920 onwards, only the power spectrum of the SLR flows exhibits a longer period ($\sim$24 year) component. The annual structure is visible in both spectra, but with striking ruptures for the Saint-Lawrence River flow (Fig. 3b). The annual component clearly disappears in 1965–1970, while intra-annual structures appear in the last two data decades (1975–1995). Note that the year—1970 has been recently identified as a possible change point in the Canadian Southeastern streamflow (Anctil and Coulibaly, 2004). Different studies have shown that the multi-annual (or low-frequency) components revealed by the wavelet analysis of streamflows can be related to climatic fluctuations (Coulibaly et al., 2000a; Anctil and Coulibaly, 2004) by performing cross-wavelet (or covariance) analysis. However, this is beyond the objective of our analysis. Here the wavelet analysis results are used to highlight the time-scale variability of the hydrological time series. The analysis results

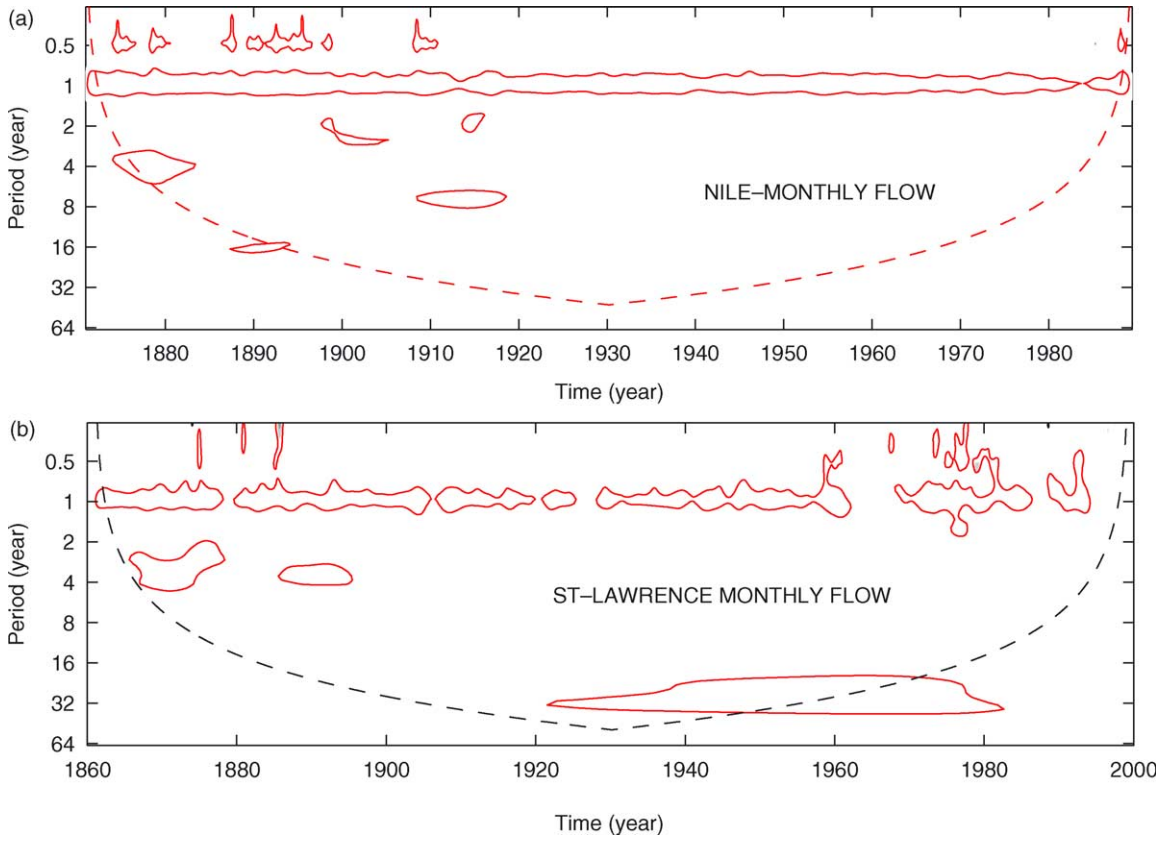

Fig. 3. (a) The local wavelet power spectrum of the Nile River monthly flow using the Morlet wavelet. The contours enclose structures of greater than 95% confidence for a red-noise process with a lag-1 coefficient of 0.90. (b) The local wavelet power spectrum of the SLR monthly flow using the Morlet wavelet. The contours enclose structures of greater than 95% confidence for a red-noise process with a lag-1 coefficient of 0.61. Other features are identical to Fig. 2b.

clearly show that the selected hydrological time series are nonstationary since their variance changes in frequency and intensity through time.

3. Ensemble of competitive dynamic recurrent neural networks

The main objective of this part of the study is to identify an optimal dynamically driven recurrent neural network (RNN) that can capture the complex time-varying structure of nonstationary hydrological series without any data pre-processing or transformation. The proposed model is essentially an ensemble of time delay RNNs (Fig. 4). The network consists of three layers: an input layer with a time delay line (TDL), a hidden layer with three independent modules (or 'subnets') of recurrent (or state) nodes, and a competitive output layer. Each sub-network (or 'subnet') contains three state nodes (selected by trial-and-error) that feed back into themselves through a set of synchronous delay lines or context units (Fig. 4). This recurrence facility confers on the subnet dynamic properties which make it possible for each module to have internal memory. The recurrent dynamic of the state neurons allows the information to be recycled over multiple time steps, and thereby to discover temporal information contained in the sequential input and that is relevant to the target function. Thus each subnet (or module) can be viewed as a single time delay RNN with an inherent dynamic memory (related to the context units) and a static memory structure (related to the input delay line). It is basically an Elman-type RNN (Elman, 1990) with an input delay line.

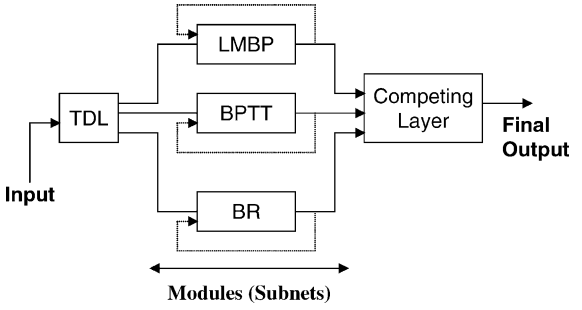

Fig. 4. Schematic of the ensemble of competitive recurrent neural networks.

Given an input variable $x(t)$, the delay line operating on $x(t)$ yields its past values $x(t-1)$, $x(t-2)$, …, $x(t-p)$ where $p=3$ is the optimal delay memory order selected by trial-and-error in this case. Therefore the input signal $s_i^{(t)}$ to a neuron i of a subnet, is given by the convolution sum

$$s_i^{(t)} = \sum_{k=0}^{p} w_i^{(k)} x^{(t-k)} + b_i = \mathrm{w}_i \mathbf{x}^{(t)} \tag{1}$$

where $\mathbf{w}_i$ is the weight vector for neuron i and $\mathbf{x}^{(t)}$ denotes the vector of delayed values from the input time delay line. It is important to note that the use of time delay in this context is different from the 'sliding or moving window' method because the input signal to the activation function consists of the convolution summation of the sequences of the input variable and synaptic weights of the neuron plus a bias b_i. More precisely, the connection weight $\mathbf{w}_\mathrm{i}$ is a vector rather than a single value as used in the sliding (or moving) window approach commonly used for temporal processing with feedforward neural networks.

The recurrence equation that defines the temporal dynamics of the RNN typically filters the weighted sum of the inputs and states through a nonlinear mapping function. This equation has the general form:

$$S^{(t+1)} = \Phi(\mathrm{I}^{(t)}, \mathrm{S}^{(t)}, \mathrm{W}, \Theta) \tag{2}$$

where $\mathbf{S}^{(t)}$ is the state vector representing the values of all the state neurons at time t, $\mathbf{I}^{(t)}$ is the input vector at time t, $\Phi(.)$ denotes a logistic function characterizing the hidden nodes, $\mathbf{W}$ is a set of weight matrices defining the weighted connections between the subnet layers, and $\boldsymbol{\Theta}$ is a set of biases on the state neurons. Note that Eq. (2) is typically a standard definition of the $\{state-input-next\text{-}state\}$ mapping found in the definitions of both finite state automata (Kohavi, 1978) and nonlinear dynamical system models (Narendra and Parthasarathy, 1990). Finally, the output of each sub-network depends not only on the connection weights and the current input signal but also on the previous states of the network, as follows

$$y_j^{(t)} = \mathrm{AS}^{(t)} \tag{3}$$

with

$$S^{(t)} = \Phi(\mathrm{W}_h \mathrm{S}^{(t-1)} + \mathrm{W}_{h_0} \mathrm{I}^{(t-1)}) \quad (4)$$

where $y_j^{(t)}$ is the output of a subnet assuming a linear output node j, $\mathbf{A}$ is the weight matrix of the output layer node j connected to the hidden neurons, the matrix $\mathbf{W}_h$ represents the weights of the h ($h=1,\ldots,3$) hidden nodes that are connected to the context units, and $\mathbf{W}_{ho}$ is the weight matrix of the hidden units connected to the input neurons. Each subnet in the network is a typical *state-space model* since (4) performs the state estimation and (3) the evaluation. Here, the RNN model is developed using the Neural Network Toolbox 3 (The Mathworks Inc., Natick, Massachusetts).

A major difficulty when using time delay RNNs is the training complexity because the computation of $\nabla E(w)$, the gradient of the error E with respect to the weights is not trivial since the error is not defined at a fixed point but rather is a function of the network temporal behavior. Here, to identify an optimal training method and also minimize the computational cost, each module (or subnet) of the network is trained with a different algorithm, in parallel, using the same delayed inputs. The network specifically makes use of (1) an adapted recursive form of the Levenberg–Marquardt backpropagation (LMBP) (Hagan and Menhaj, 1994), (2) a variant of backpropagation through time (BPTT) (Williams and Peng, 1990) which is considered the best on-line technique for practical problems (Pearlmutter, 1995); and (3) a variation of the Bayesian regularization (BR) method (Jones and MacKay, 1998).

Finally, the competitive output layer stores all the outputs of the subnets, computes a vector of probabilities for each subnet, and selects the output that has the maximum probability of being correct given the target pattern. The output layer is similar to the competitive output layer used in probabilistic neural networks (Coulibaly et al., 2001). The performance of the optimal (or 'winning') network is assessed using the root mean squared error (RMSE) and the model efficiency index (R^2) (Nash and Sutcliffe, 1970). Given that all the outputs are automatically stored, comparative performance study can also be completed. To further assess the forecast improvement obtained with the optimal RNN model as compared to the best MARS model, a mean error decrease (MED) is used. The MED is the average decrease (%) in the RMSE of the optimal RNN model as compared to the best MARS model. The MED is also referred to herein as the model forecast improvement.

Two model calibration experiments are performed using two different methods for data division (i.e. split-sampling). First, the proposed network is trained (or calibrated) using about 95% of each of the hydrological data, and the validation is performed on the last 5 years of each series. The same calibration and validation sets are used for the benchmark model (MARS) identification and evaluation, also applied, for model performance comparison purposes, in this study. Secondly, to further evaluate the performance of the proposed method, cross-validation is used to increase the training and prediction samples. In this case, a cross-validation with stopped training approach is used to evaluate the model performance. A generalization loss criterion (Coulibaly et al., 2000b) is used to stop network training. Given that the generalization error is estimated by cross-validation with a holdout data set (used to evaluate the effectiveness of the stopping criterion), this allows for comparing solutions and stopping when the validation error is effectively optimal. The practical objective is to provide long-term (12 month-ahead) prediction of monthly flows and bi-weekly lake volumes. The temporal distribution of flow and volume throughout the year is particularly important for water resources planning and management.

4. Results and discussion

The root mean square error (RMSE) and the model efficiency index (R^2) are used to evaluate the model performance. In general, a R^2 value greater than 0.9 indicates a very satisfactory model performance, while a R^2 value in the range 0.8–0.9 indicates an acceptable (or good) model, and values less than 0.8 indicate an unsatisfactory model. Note that only the 12-month-ahead predictions are of concern as specified in the previous section, and are thus analyzed in detail hereafter. Fig. 5 shows the average R^2 index statistics for the validation period 1995–1999 for the SLR and GSL, and 1985–1989 in the case of the Nile

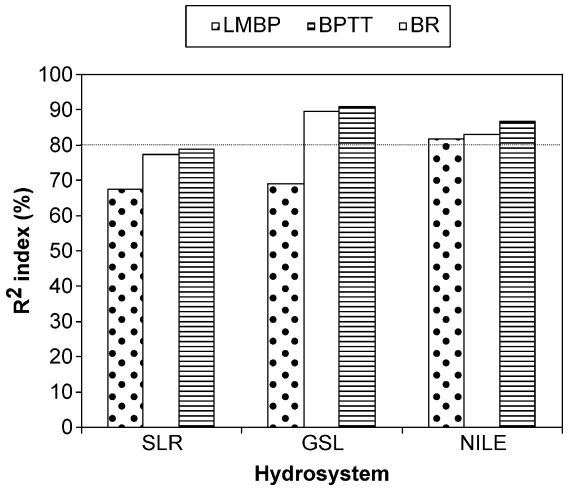

Fig. 5. Comparative model efficiency index for the three subnetworks.

River. From Fig. 5, it can be seen that the optimal methods for modeling the three complex time series are the RNN trained with either the BR or the truncated BPTT. However, the overall best training algorithm appears to be the BR. The recursive LMBP appears to be the least suitable for modeling the three time series. These results indicate that the performance of even powerful online RNN training methods can be case dependent. A salient advantage of the proposed ensemble competition RNN method is that it can directly identify the optimal RNN model for each hydrological time series in any case. Furthermore, the ensemble competition approach significantly reduces ($\sim$60%) the computing time as compared to an individual training of each subnet. However, it appears that for the SLR flows, even the optimal algorithm (BR) does not provide good forecasts (since $R^2 < 0.8$). This may be due to the more complex nonstationary structure of the SLR flows characterized by periodic ruptures of the annual process (Fig. 3b). For the GSL volume prediction, the BPTT and BR algorithms provide slightly similar and good results ($0.8 < R^2 \leq 0.9$), while the LMBP is clearly inefficient in this case. The Nile River flows can be effectively predicted by any of the three algorithms (Fig. 5). However the best model still appears to be the RNN trained with BR (termed RNN-BR) whatever the system in this case. The poor performance of the recursive LMBP may be due to the complex and inaccurate approximation of the second order derivatives. These results may also indicate that the LMBP is less suitable for time delay RNN training than the BR and the BPTT algorithms.

Thus, the ensemble competition approach automatically selects the optimally trained network, and thereby provides the best results for each hydrological time series being modeled. To further assess the performance of the proposed method, the best RNN model identified (namely RNN-BR) is compared to an optimal MARS model using the corresponding validation RMSE and R^2 statistics (Table 1). The MARS model is developed using S-PLUS Software (Insightful Corporation, Seattle, Washington) and the same calibration and validation datasets used with the RNN model. It appears from Table 1 that the optimal RNN model outperforms the MARS model for all the three time series. For the GSL storage volumes, the optimal RNN model (RNN-BR) and the best MARS model have respectively a R^2 index value of 0.91 and 0.87, indicating that the RNN-BR model provides 'very satisfactory' forecasts while the MARS model

Table 1
Model validation statistics for the 12-month-ahead predictions

Model	GSL volumes mean: 19.557×10^9 m^3			Nile River flows mean: 6.9765×10^9 m^3/month			SLR flows mean: 7528 m^3/s		
	RMSE (10^9 m^3)	R^2	MED (%)	RMSE (10^9m^3/month)	R^2	MED (%)	RMSE (m^3/s)	R^2	MED (%)
RNN-BR	0.70	0.91	53	2.43	0.86	64	455	0.78	41
MARS	1.49	0.88		6.90	0.64		770	0.31	

RNN-BR, Recurrent neural networks with Bayesian regularization; MARS, multivariate adaptive regression splines; RMSE, root mean square error; R^2, model efficiency index, MED, mean error decrease; GSL, Great Salt Lake; SLR Saint-Lawrence River.

results are 'fairly acceptable'. However, for the Nile River flows, the RNN-BR and the MARS are respectively 'fairly acceptable' ($R^2=0.86$) and 'unsa-unsatisfactory' ($R^2=0.64$). Conversely, for the SLR flows, none of the proposed methods are satisfactory ($R^2<0.8$). However, the RNN-BR prediction RMSE is less than 10% of the mean monthly flow of the SLR for the validation period (Table 1), while the MARS model RMSE for the SLR flows is about twice that of the optimal RNN. This clearly indicates a good potential of the dynamic RNN for complex hydrological time series forecasting assuming that an appropriate training method is found. To further evaluate the prediction performance of the ensemble competition approach, cross-validation with stopped training approach is used. In this case, the number of hidden nodes is increased to six for each subnet to ensure network flexibility and avoid poor local optima. The optimal model identified remains the RNN-BR, but surprisingly there is no significant improvement of the prediction performance as compared to the conventional data division (split-sampling) approach. Therefore, the results of this experiment are not provided here. Indeed, the cross-validation approach is computationally intensive despite the use of the early-stopping, and it should perhaps be borne in mind that this approach compromises the 'independence' of the validation concept.

In general, the optimal RNN provides significant forecast improvement in terms of mean error decrease (MED) (Table 1), exceeding 40% for all three series as compared to the corresponding values of the best MARS model. For the GSL volumes and the Nile River flows, the average forecast improvement is about 53 and 64%, respectively, while for the SLR flow, the average forecast improvement is about 41%. However, despite the significant improvement of the SLR flow forecasts, the prediction results remain poor ($R^2=0.78$). This may indicate that additional explanatory variables (e.g. precipitation, climatic indices) should be included. In this case, the ensemble competition approach appears particularly useful to assess the system complexity before resorting to the provision of additional information.

To further assess the model prediction accuracy, plots of observed and predicted flow for the SLR are shown in Fig. 6. Neither the RNN-BR nor the MARS

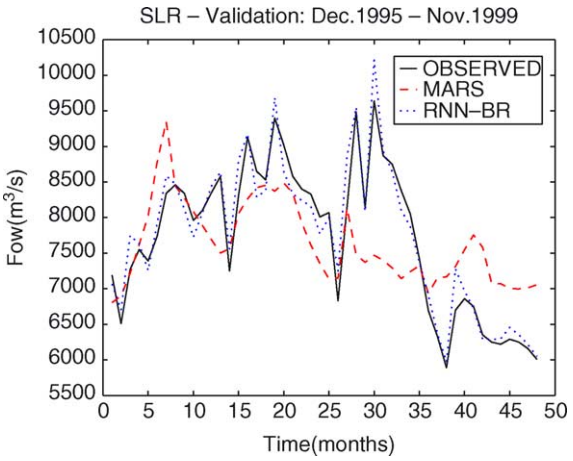

Fig. 6. Observed and predicted SLR monthly flows (Dec. 1995–Nov. 1999).

perform very well particularly for peak flows. However, it appears that the RNN-BR model performs well for low flow prediction as compared to the MARS model. Although neither of the two models provide very good flow forecasts, it appears that the proposed method has a considerable potential for an improved long-term (12-month-ahead) forecast of the SLR flows. It is anticipated that the use of additional information such as precipitation and El-Niño (ENSO) indices would improve the model prediction performance. The GSL storage volumes and Nile River flows are shown in Figs. 7 and 8, respectively.

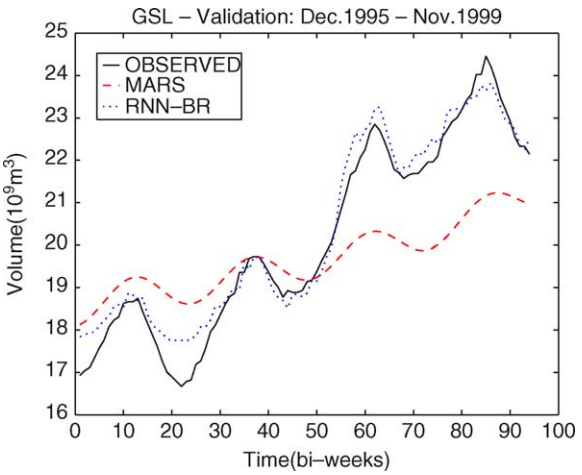

Fig. 7. Observed and predicted GSL bi-weekly volumes (Dec. 1995–Nov. 1999).

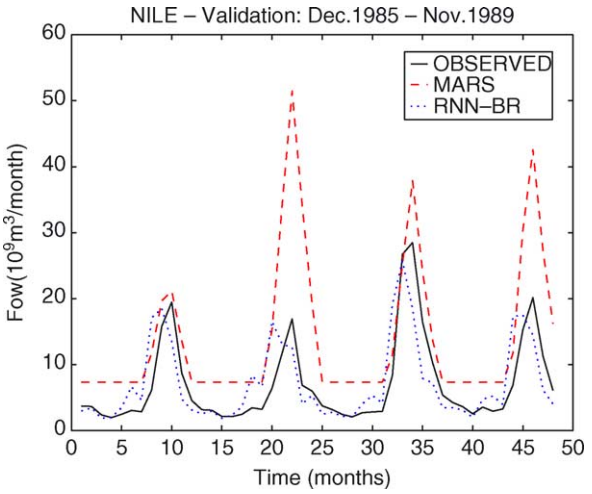

Fig. 8. Observed and predicted Nile River monthly flows (Dec. 1985–Nov. 1989).

It appears that the RNN-BR performs very well for high as well as low lake volumes (Fig. 7) as compared to the MARS model. For the Nile River flows (Fig. 8), the proposed method is less accurate in predicting the peak flows than the low flows. As regards the other two cases, the RNN-BR model appears to be significantly better than the MARS model for the modeling of the Nile River flows.

To summarize, the optimal model directly identified provides significant forecast improvement over the MARS model in a dramatically reduced ($\sim$60% less) computational time. Therefore, the proposed method can be a good practical alternative for the modeling of complex hydrological systems. The proposed approach can be extended to include more recent RNN training algorithms such as the real-coded genetic algorithm (Blanco et al., 2001), and/or the extended Kalman filter method (Sum et al., 1999). Furthermore, it could also be improved by considering recently proposed data division techniques (Bowden et al., 2002), as well as additional explicative input variables.

5. Conclusions

An optimally trained dynamic RNN can be an effective method for modeling nonstationary hydrological time series. The proposed method allows a fast identification of an optimal time delay RNN model for complex hydrological system modeling. The optimum RNN-based model proposed in this study shows very promising results for improving nonstationary hydrological time series forecasting without any data preprocessing. Significant improvements are shown in the GSL storage volume and the Nile River flow forecasts as compared with those of the MARS model. However, the optimal RNN model does not provide satisfactory forecasts for the SLR flows, indicating that additional explicative variables should be considered in this case. The study clearly shows a promising potential of the dynamic RNN method in this context. Furthermore, it is anticipated the method could be improved by including exogenous explicative input variables such as low-frequency climatic indicators, as well as by considering other recent RNN training algorithms and data division techniques.

Acknowledgements

Part of this study was funded by a grant from the Natural Sciences and Engineering Research Council of Canada to the first author. The authors would like to thank two anonymous reviewers for their valuable comments and suggestions.

References

American Society of Civil Engineers (ASCE) Task Committee on Application of Artificial Neural Networks in Hydrology, 2000. Artificial neural networks in hydrology, II, hydrologic applications. J. Hydrol. Eng. ASCE 5 (2), 124–137.

Anctil, F., Coulibaly, P., 2004. Wavelet analysis of the interannual variability in Southern Quebec streamflow. J. Climate 1, 163–173.

Bernier, J., 1994. Statistical detection of changes in geophysical series, in: Duckstein, L., Parent, E. (Eds.), Engineering Risk in Natural Resources Management. Kluwer, Dordrecht, The Netherlands, pp. 159–176.

Blanco, A., Delgado, M., Pegalajar, M.C., 2001. A real-coded genetic algorithm for training recurrent neural networks. Neural Netw. 14, 93–105.

Bowden, G.J., Maier, H.R., Dandy, G.C., 2002. Optimal division of data for neural network models in water resources applications. Water Resour. Res. 38 (2), 2–11.

Box, G.E.P., Jenkins, G.M., 1976. Time Series Analysis: Forecasting and Control Holden-Day, San Francisco, CA, USA 1976.

Coulibaly, P., Anctil, F., Bobée, B., 1999. Hydrological forecasting using artificial neural networks: The state of the art. Can. J. Civ. Eng. 26 (3), 293–304.

Coulibaly, P., Anctil, F., Rasmussen, P.F., Bobée, B., 2000a. A recurrent neural networks approach using indices of low-frequency climatic variability to forecast regional annual runoff. Hydrol. Process. 14 (15), 2755–2777.

Coulibaly, P., Anctil, F., Bobée, B., 2000b. Daily reservoir inflow forecasting using artificial neural networks with stopped training approach. J. Hydrol. 230, 244–257.

Coulibaly, P., Anctil, F., Aravena, R., Bobée, B., 2001. Artificial neural network modeling of water table depth fluctuations. Water Resour. Res. 37 (4), 885–897.

Daubechies, I., 1990. The wavelet transform time-frequency localization and signal analysis. IEEE Trans. Inform. Theory 36, 961–1004.

Elman, J.L., 1990. Finding structure in time. Cogn. Sci. 14, 179–211.

Eltahir, E.A.B., 1996. El-Niño and the natural variability in the flow of the Nile River. Water Resour. Res. 32 (1), 131–137.

Foufoula-Georgiou, E., Kumar, P., 1995. Wavelets in Geophysics. Academic Press, New York.

Friedman, J.H., 1991. Multivariate adaptive regression splines. Ann. Stat. 19, 1–141.

Giles, C.L., Lawrence, S., Tsoi, A.C., 1997. Rule inference for financial prediction using recurrent neural networks, Proceedings of the IEEE/IAFE Conference on Computational Intelligence for Financial Engineering. IEEE Press, Piscataway, NJ pp. 253–259.

Hagan, M.T., Menhaj, M.B., 1994. Training feedforward networks with Marquardt algorithm. IEEE Trans. Neural Netw. 5 (6), 989–993.

Haykin, S., 1999. Neural Networks: A Comprehensive Foundation. Prentice-Hall, Upper Saddle River, NJ.

Haykin, S., Li, L., 1995. Nonlinear adaptive prediction of nonstationary signals. IEEE Trans. Signal Process. 43 (2), 526–535.

Iatrou, M., Berger, T.W., Marmarelis, V.Z., 1999. Modeling of nonlinear nonstationary dynamic systems with a novel class of artificial neural networks. IEEE Trans. Neural Netw. 10 (2), 327–339.

Jones, C.A.L., MacKay, D.J.C., 1998. A recurrent neural network for modeling dynamical systems. Comput. Neural Syst. 9, 531–547.

Kohavi, Z., 1978. Switching and Finite Automata Theory. McGraw-Hill, New York.

Labat, D., Ababou, R., Mangin, A., 2000. Rainfall-runoff relations for karstic springs. Part II: continuous wavelet and discrete orthogonal multiresolution analyses. J. Hydrol. 238, 149–178.

Lall, U., Mann, M., 1995. The Great Salt Lake: a barometer of low-frequency climatic variability. Water Resour. Res. 31 (10), 2503–2515.

Lall, U., Sangoyomi, T., Abarbanel, H.D.I., 1996. Nonlinear dynamics of the Great Salt Lake: Nonparametric short-term forecasting. Water Resour. Res 32 (4), 975–985.

Maier, H.R., Dandy, G.C., 2000. Neural networks for the prediction and forecasting of water resources variables: a review of modelling issues and applications. Environ. Model. Software 15, 101–124.

Mann, E., Lall, U., Saltzman, B., 1995. Decadal-to-centenial-scale climate variability: insights into the rise and fall of the Great Salt Lake. Geophys. Res. Lett. 22 (8), 937–940.

Narendra, K., Parthasarathy, K., 1990. Identification and control of dynamical systems using neural networks. IEEE Trans. Neural Netw. 1, 4–27.

Nash, J.E., Sutcliffe, J.V., 1970. River flow forecasting through conceptual models. Part I: a discussion of principles. J. Hydrol. 10, 282–290.

Pearlmutter, B.A., 1995. Gradient calculations for dynamic recurrent neural networks: a survey. IEEE Trans. Neural Netw. 6 (5), 1212–1228.

Saad, E.W., Prokhorov, D.V., Wunsch, D.C., 1998. Comparative study of stock trend prediction using time delay, recurrent and probabilistic neural networks. IEEE Trans. Neural Netw. 9 (6), 1456–1470.

Sangoyomi, T.B., 1993. Climatic Variability and Dynamics of Great Salt Lake Hydrology, PhD dissertation, Utah State University, Logan, UT, pp. 247.

Sum, J., Leung, C., Young, G.H., Kan, W., 1999. On the Kalman filtering method in neural network training and pruning. IEEE Trans. Neural Netw. 10 (1), 161–166.

Torrence, C., Campo, G.P., 1998. A practical guide to wavelet analysis. Bull. Am. Meteor. Soc. 79, 61–78.

Williams, R.J., Peng, J., 1990. An efficient gradient-based algorithm for on-line training of recurrent network trajectories. Neural Comput. 2, 490–501.

Young, P.C., 1999. Nonstationary time series analysis and forecasting. Progress Environ. Sci. 1, 3–48.